DL/SCI/TM41A

technical memorandum Daresbury Laboratory

DL/SCI/TM41A

BEAM POSITION MONITORS FOR THE HIGH BRIGHTNESS LATTICE

by

T. RING, Daresbury Laboratory

JUNE, 1985

RING-85/134

Science & Engineering Research Council

Daresbury Laboratory

Daresbury, Warrington WA4 4AD

1. INTRODUCTION

Engineering developments associated with the high brightness lattice[1] and the projected change in machine operating parameters will inherently affect the diagnostics systems and devices installed at present in the storage ring. This is particularly true of the beam position monitoring (BPI) system.

The present system[2] of monitors distributed around the storage ring is, in some respects, a compromise solution to the problem of measuring vertical and horizontal closed orbit. Combined function monitors which respond on both the vertical and horizontal axis were originally installed in each of the sixteen machine straight sections. This system satisfied the basic requirement of providing, in the present 8 unit cell FODO lattice, more than four monitor positions per betatron wavelength in both the radial and vertical planes but, because of space constraints in the original design of machine straight, two monitors have been lost following subsequent installation of Wiggler and Undulator magnets. Space constraints in the original design have also resulted in an almost random positioning of BPI's in the machine straight sections so that beam position in both planes is now monitored at points which vary relative to the β function. Finally, the proximity of beamlines in three machine straights has resulted in non-standard monitors (45° displaced axis) being fitted in those straights.

The new sixteen unit cell lattice with its higher betatron tune values and the limited space available in the redesigned machine straights for fitting standard BPI vessels forces a fundamental re-evaluation of the beam position monitor system. The design aims for the new system are based on accepting the space limitations imposed while still providing the monitor points required to give good radial and vertical closed orbit plots.

2. THE HBL SYSTEM

The new lattice will achieve an improvement in source brightness by the introduction of a second quadrupole magnet (D type) into the upstream end of each machine straight section. The arrangement of the focusing quadrupoles and the beam steering magnets in the redesigned straight is shown in fig.1 together with the lattice β function.

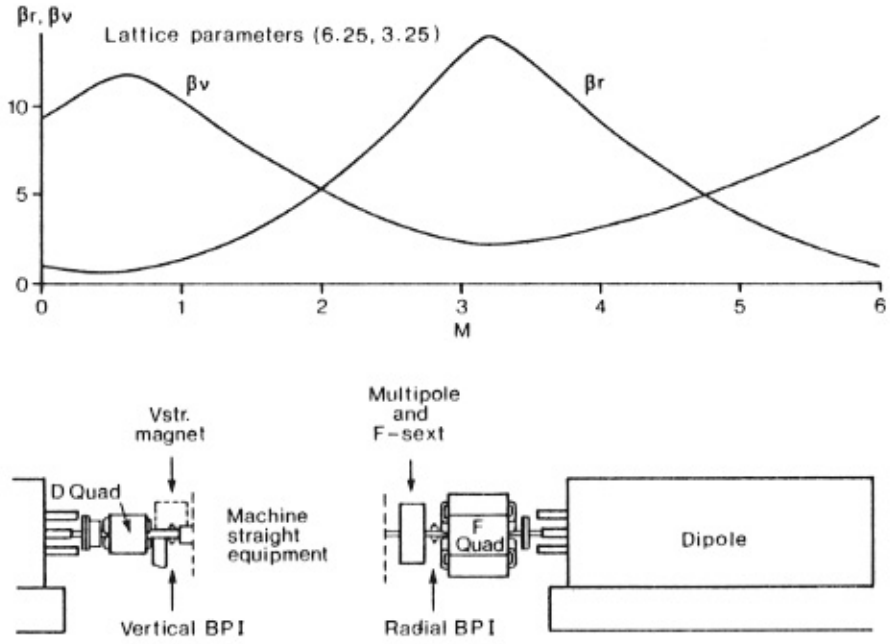

Fig.1. Location of BPI's in Machine Straight

Standard F and D quadrupole sections will be installed in each machine straight with a single function BPI mounted local to each quadrupole. Each monitor will measure beam displacement in the focusing direction of the adjacent quadrupole and is thus, as shown in fig.1, located near the corresponding β maximum point. This provides maximum sensitivity for detecting radial and vertical betatron oscillations (Qr,Qv).

Mounting the BPI assemblies as an integral part of a quadrupole vacuum vessel means that the BPI is no longer a separate and demountable unit and also that the vessel geometry is very much smaller than the 200mm diameter circular section used in the present machine. Both these factors influence the type of pick-up electrode to be used and make the quarter wave stripline coupler an unsuitable device for use in the new lattice. The internal assembly of a scaled down stripline electrode would be very complex and the high sensitivity of a practical stripline would result in excessive power being coupled from each measurement port. A more practical alternative is to use a capacitive button type pick-up.

A feature of the SRS is that the vacuum vessel does not maintain a uniform cross section through the machine straight. The geometry of the vessel at the F and D quadrupoles will differ considerably and in neither case will

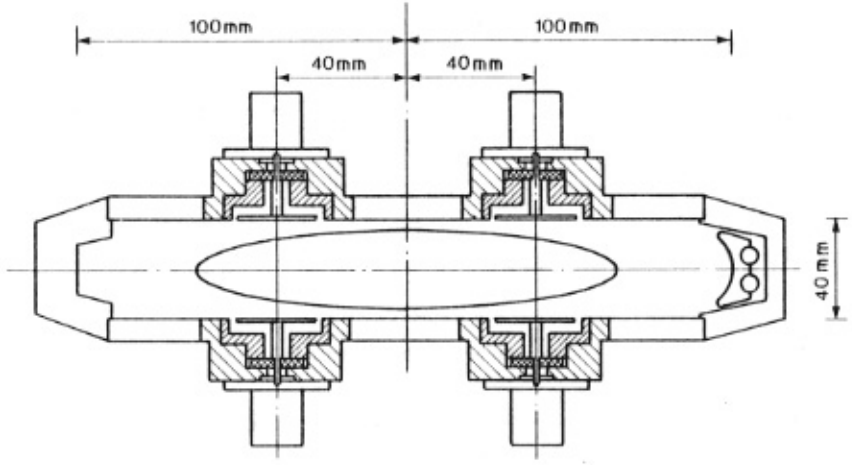

Fig.2. 'F' Vessel BPI

the BPI assembly provide a close approximation to the well documented[3] elliptical section BPI often adopted as a standard. A simplified outline of the proposed F-quadrupole BPI assembly is shown in fig.2.

An assembly containing four button electrodes, each 25mm diameter, will be used to monitor horizontal beam displacement in the F vessel. Each electrode is fabricated to form part of a vacuum coaxial feedthrough assembly which is then welded into the quadrupole vacuum vessel. Because the electrode is then an integral and non-demountable part of the quadrupole vessel it is planned to provide the facility for removing the type N output connector and capping the feedthrough in the event of a vacuum leak developing during machine operation.

The cross section of the BPI assembly used to monitor vertical beam displacement in the D vessel is considerably different as shown in outline form in fig.3.

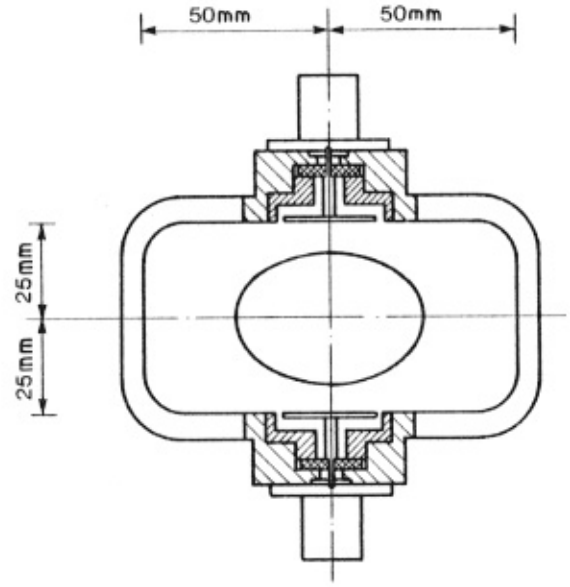

Fig.3. 'D' Vessel BPI

The vessel will provide little free space for mounting the button electrodes yet the monitor must provide, within the limited vertical aperture available, a good response to beam displacements over a minimum range of ±15mm. Preliminary investigations of monitor response indicated that the best performance in the D vessel would be achieved using two button electrodes mounted on the centre vertical axis of the vessel.

Additional investigations, including laboratory model tests, have been carried out to optimise monitor response within the vessel geometries available in the HBL and to assess the sensitivity of the capacitive buttons as beam pick-ups.

3. MONITOR RESPONSE

The vessels incorporating the BPI pick-ups are unusual in that they are rectangular in section with, in the case of the F-quadrupole beam position monitor, a somewhat extreme 'letterbox' geometry. The expected response of a rectangular section BPI is first considered.

3.1 The Coupling Impedance of a Button Pick-up

Consider a single button pick-up mounted flush with the surface of a rectangular vessel (shown in fig.4): the vessel geometry proposed for the HBL

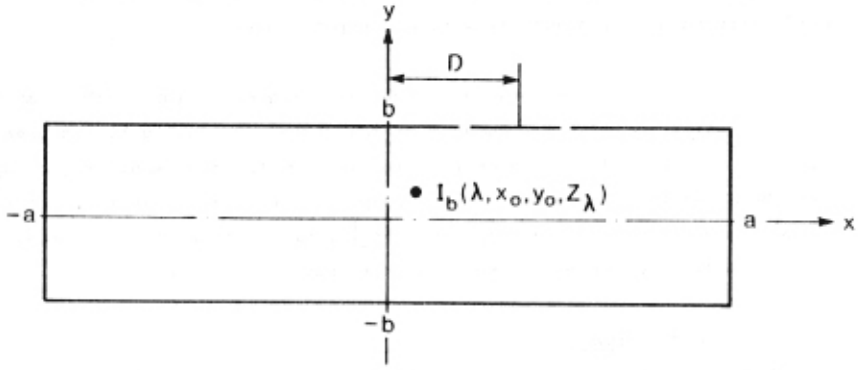

Fig.4. Vessel geometry and beam coordinates

If the plate is coupled directly to a terminated coaxial line of impedance Z_o then it can be shown (Appendix 1) that the coupling impedance Z_c of the pick-up is:-

a) When $\omega_\lambda Z_o C_p < 1$

ω_λ = Angular Frequency of the Fourier beam component, wavelength λ

C_p = Capacitance of the plate assembly.

$$Z_c = \frac{2\pi s}{\lambda a} Z_o \sum_{m=1}^{\infty} \beta_{m(x = D)} \qquad (1)$$

b) When $\omega_\lambda Z_o C_p > 1$

$$Z_c = \frac{s}{C_{p\,av}} \sum_{m=1}^{\infty} \beta_{m(x = D)} \qquad (2)$$

where: s = surface area of plate

v = particle beam velocity in Z direction

and:
$$\beta_{m(x)} = \frac{\sin\left[\frac{m\pi(a+x_o)}{2a}\right] \; sh\left[\frac{m\pi(b+y_o)}{2a}\right]}{sh\left[\frac{m\pi b}{a}\right]} \sin\left[\frac{m\pi(a+x)}{2a}\right]$$

This pick-up response takes the form of a single pole high pass filter (fig.5) with a breakpoint:

$$f_c = \frac{1}{2\pi Z_o C_p}$$

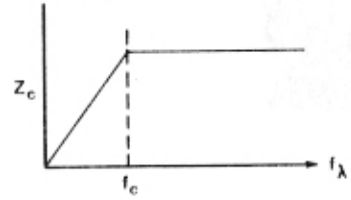

$$Z_c = \frac{s}{C_{p\,av}} \sum_{m=1}^{\infty} \beta_{m(x = D)} \qquad (f_\lambda > f_c)$$

Fig.5. Frequency response of a pick-up button

Two observations can be made about the response of a button pick-up:

(1) If a wide band beam diagnostics pick-up is required, the break point frequency f_c should be below the fundamental r.f. beam component. This can be achieved by inserting a ceramic spacer in the button assembly to increase the plate capacitance C_p. A flat wide band response covering beam harmonics to an upper frequency limited by vessel cut-off will then be achieved.

(2) If the button is one of the pick-ups in a beam position monitor operating in a narrow frequency band centred on the fundamental r.f. beam component, the break point frequency f_c should be above the working frequency of the monitor. A low capacitance, air spaced button is required. The monitor response is then less dependent on extreme precision in the internal assembly of the pick-up and is simply determined by an accurately defined surface area S and calibrated terminating impedance Z_o.

Mounting a model button pick-up plate in a wide band coaxial test assembly demonstrated the effectiveness of the button pick-up as a wide band monitor (fig.6).

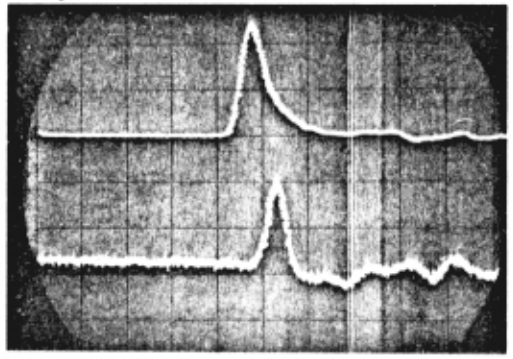

TOP:

Drive pulse = 130ps (FWHM)

BOTTOM:

Plate output, dia. = 25mm

$C_p \simeq 5pf$

Fig.6. Pulse response of a pick-up button

3.2 The F-Quadrupole BPI

The F-quadrupole BPI is mounted in a vessel with an extreme 'letterbox' geometry so this case was chosen to check the validity of the expression

(eqn.(1)) for plate coupling impedance Z_c. The basic geometry of a laboratory model F-quadrupole BPI is shown in fig.7.

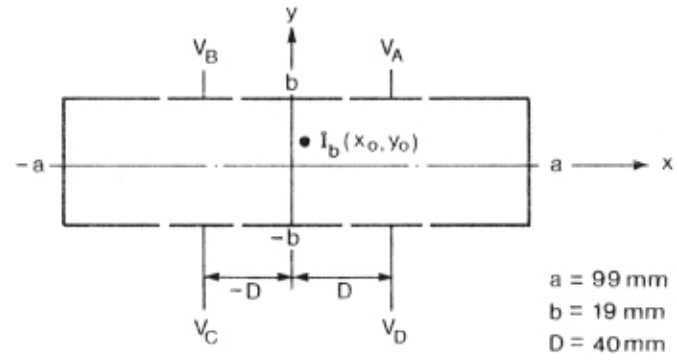

Fig.7. Model F-quad Vessel Geometry

The four pick-ups in the model BPI were air spaced 25mm diameter buttons.

3.2.1. Measured response

The model BPI was mounted in a calibration rig in which the BPI vessel formed part of a matched coaxial test assembly with a centre conductor to represent the beam. Calibration was caried out using a 500 MHz test signal to simulate the fundamental r.f. beam component in the SRS and a set of 500 MHz hybrids were used to process the monitor output signals.

The measured response obtained is shown in response plot 1 (shown at end of report) which includes a schematic of the signal processing hybrid used to derive the sum (Σ) and difference (Δ) signals from the four monitor pick-ups. It may be noted that the total current response, represented in terms of an average or composite coupling impedance $|Z_c|$ from the four pick-up plates, varies considerably across the horizontal measurement aperture.

3.2.2. Computed response

Taking the same geometry vessel, computer processed sum (Σ) and differ-

ence (Δ) signals were derived using the relationships:

$$\Sigma_{x_o} = V_A + V_B + V_C + V_D$$

$$\Delta_{x_o} = (V_A + V_D) - (V_B + V_C)$$

where the plate output voltages are obtained using the derived expression for plate coupling impedance: eqn.(1) as $f_c >> 500$ MHz

then:

$$V_A = I_b \frac{2\pi s}{\lambda a} Z_o \sum_{m=1}^{\infty} \beta_{m(x = D)}$$

$$V_D = I_b \frac{2\pi s}{\lambda a} Z_o \sum_{m=1}^{\infty} \beta_{m(x = D)} \qquad \text{where } -y_o \text{ is substituted for } y_o$$

$$V_B = I_b \frac{2\pi s}{\lambda a} Z_o \sum_{m=1}^{\infty} \beta_{m(x = -D)}$$

$$V_C = I_b \frac{2\pi s}{\lambda a} Z_o \sum_{m=1}^{\infty} \beta_{m(x = -D)} \qquad \text{where } -y_o \text{ is substituted for } y_o$$

The BPI response $\frac{\Delta x_o}{\Sigma x_o}$ and the composite coupling impedance:

$\left|Z_c\right| = \frac{\Sigma x_o}{4I_b}$ was plotted.

The resultant plots are shown in response plot 2 (shown at end of report) for the particular case of a beam with zero vertical offset ($y_o = o$). For comparison, and to confirm the general validity of the derived expression for monitor coupling, a number of the corresponding measurement points from response plot 1 are also shown. Within the limits of accuracy provided by the fabricated model BPI and an uncalibrated set of signal processing hybrids, the general agreement is good.

3.3 The D-Quadrupole BPI

Similar work was carried out on a laboratory model D-quadrupole BPI with the basic geometry shown in fig.8.

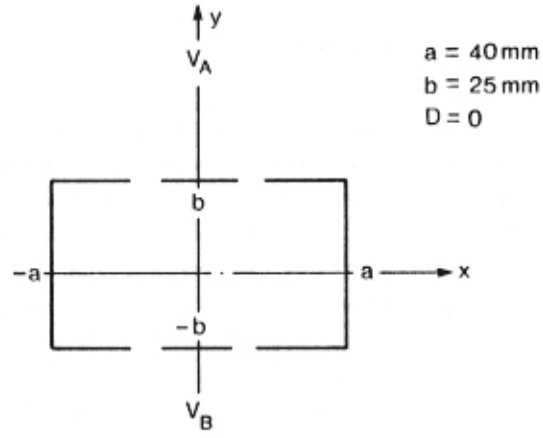

Fig.8. Model D-Quad Vessel Geometry

The model BPI incorporated two rectangular air spaced pick-up plates (7 × 25mm) on the central vertical axis. The measured response is shown in response plot 3 (see end of report) which also shows a schematic of the signal processing hybrid.
The computed response was plotted using the relationships:

$$\Sigma y_o = V_A + V_B$$

$$\Delta y_o = V_A - V_B$$

where

$$V_A = I_b \frac{2\pi s}{\lambda a} Z_o \sum_{m=1}^{\infty} \beta_{m(x = o)}$$

$$V_B = I_b \frac{2\pi s}{\lambda a} Z_o \sum_{m=1}^{\infty} \beta_{m(x=0)} \qquad \text{where } -y_o \text{ is substituted for } y_o$$

The BPI response $\frac{\Delta y_o}{\Sigma y_o}$ and the composite coupling impedance:

$$|Z_c| = \frac{\Sigma y_o}{2I_b}$$ were derived.

The plots shown in response plot 4 (shown at end of report) were those obtained following a number of computer simulations carried out to optimise the size of the pick-up plates. In this particular case, the pick-up buttons were 15mm diameter circular plates. For comparison a number of the corresponding measurement points from response plot 3 are also shown, the measured values for $|Z_c|$ being linearly scaled to the new plate dimensions.

3.4 The Beam Absorber

The model tests confirm that capacitive pick-up buttons installed as an integral part of the rectangular section vacuum vessels at the F and D quadrupoles can provide an effective BPI response. However, in each case the vessel will also incorporate a water cooled absorber which will modify the internal geometry of the vessel so additional computer simulations were carried out to assess its implications on BPI monitor design.

In the case of the F-quadrupole vessel, the cooled absorber introduced an effective shift of 10mm in the position of one side wall in the vessel assembly. Computer response plots confirmed that this degree of vessel offset introduced an error in the centre zero measurement position of less than 0.1mm and virtually no change in the BPI response over a central ± 25mm measurement region. The effect of the cooled absorber in the F-quadrupole vessel can safely be ignored.

The cooled absorber mounted in the D-quadrupole vessel had, however, a significant effect on vessel geometry and corresponding response plot as the horizontal aperture on one side of beam centre was reduced to 25mm. The

final design of D-quadrupole BPI vessel incorporates a cooled absorber fabricated to form a vessel side wall 25mm away from beam centre and a dummy side wall position 25mm on the opposite side of beam centre.

The resultant plots for a beam with zero horizontal offset ($x_o = 0$) and 10mm horizontal offset ($x_o = 10$mm) are shown in response plots 5 and 6 respectively. These response plots indicate that there is some reduction in linearity over the central working aperture and that there is now a greater variation in the coupling impedance response. However, the change in vessel geometry has not seriously compromised monitor operation and it still provides a useful working aperture in excess of ±15mm.

4. IMPLEMENTING THE SYSTEM IN THE SRS

4.1 General Observations

In addition to providing the basic response and sensitivity data required when introducing the new system of ring BPI's into the SRS, the above tests allow a number of interesting observations to be made.

In particular, the tests verify that the method currently in use in the SRS, of directly processing the sum (Σ) and difference (Δ) monitor signals using a set of passive stripline hybrids is equally valid for the proposed capacitive button monitors. The Laboratory model tests also show that both the model BPI assemblies produce a low value calibration factor where this is defined as:

$$x = C_x \frac{\Delta x_o}{\Sigma x_o} \qquad y = C_y \frac{\Delta y_o}{\Sigma y_o}$$

where:

C_x and C_y : calibration factors of the F and D monitors respectively
x and y : beam displacement in mm in the F and D monitors respectively.

The significance of both these observations is illustrated when the offset and calibration errors introduced by the subsequent signal processing and display system are considered. Consider the case of the F-quadrupole BPI:

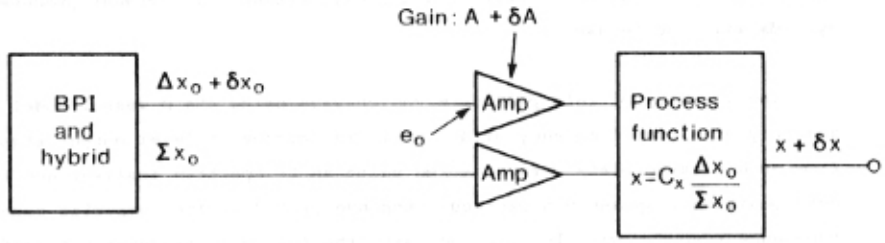

Fig.9. Signal Processing Offset and Calibration Errors

Figure 9 is a simplified representation of the source of measurement error in the signal processing system. The BPI and hybrid introduce a centre zero offset error δx_o, there is a differential error in channel gain of δA and the signal processing system introduces an input offset voltage of e_o. The resultant error in processed beam position (δx.mm) is then:

$$\delta_x = \frac{C_x}{\Sigma x_o}\left(1 + \frac{\delta A}{A}\right)(\delta x_o + e_o) + \frac{\delta A}{A}\,x \qquad (3)$$

The first term in eqn.(3) defines the zero offset error and the second term simply represents the channel calibration accuracy.

It will be noted that, given $\delta A << A$, the centre zero offset error is largely independent of channel amplifier gain and differential gain error. Thus the stability of the zero offset in a hybrid based system is largely unaffected by the many factors which determine the accuracy and stability of signal channel gain in a practical signal processing system. These include the stability of the amplifier and signal processing electronics and also the variations in cable attenuation and insertion loss which will occur in any signal switching multiplexer system.

It will also be noted that the centre zero offset error defined by eqn. (3) is directly proportional to the calibration factor C_x. The calibration factor thus asumes a more useful role as a measure of monitor performance or quality factory. The lower the value of C_x the better is monitor performance.

The measured values for C_x and C_y (14 and 18 respectively) presented by the new monitors compare well with the calibration factor ($C_x = C_y = 52$) of the installed stripline monitors and indicate a potential for a reduction in processed measurement centre error.

4.2 Implementation

The factors discussed above and the general test results obtained indicate that the new monitors are compatible with the present signal processing and display system installed in the storage ring. Essentially, the new system of BPI's can be considered a plug-in replacement for the present stripline beam position monitors.

The installed system of coaxial relays, the BPI signal multiplexer, can be used to switch the signals from the two monitors in each straight into a set of four high quality cables for subsequent signal processing at a central monitoring station. The signal display and readout system located in the monitoring station is shown in fig.10.

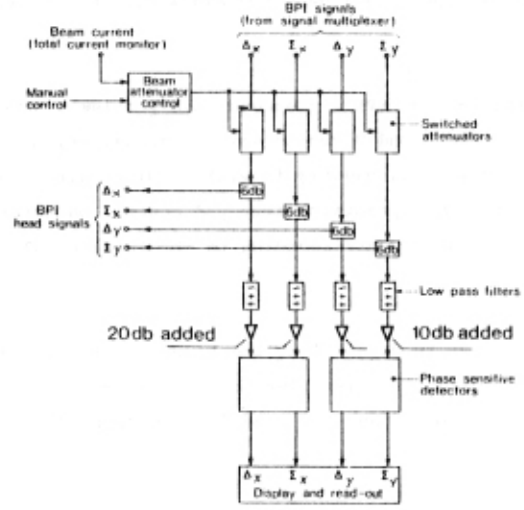

The main components in this system are the phase sensitive detectors which, operating at frequencies centred on the 500 MHz fundamental beam com-

ponent, are used to detect the Σ and Δ signals from each monitor. The single modification required to be made to the present installed system is the addition of the 10dB and 20dB amplifiers shown at the inputs of the two phase sensitive detectors. These amplifiers compensate for the lower signal levels (reduced coupling impedance Z_c) obtained from the button pick-ups.

Measurements of performance indicate that, at present, the signal processing system introduces offset errors of less than ± 0.5mm and that variations in signal channel gain due to signal switching and phase errors in the cable network introduce calibration errors of < ± 3%. This last figure will not be changed following the installation of the new monitors but a significant improvement in zero offset error is expected. The lower value calibration factor (C_x and C_y) should reduce the zero offset to a value approaching ± 0.1mm (< ± 0.2mm).

Other aspects of system performance will be essentially unchanged. Operation should be maintained down to a level of stored beam current of 10mA and the system will provide a detected bandwidth of approximately 50 MHz.

4.3 Monitor Calibration

Calibrating the new BPI's presents some problems. The monitors are an integral part of the F and D vesels which, themselves, do not present a uniform cross section. Consequently it will be difficult to assemble a matched coaxial test rig with a precision surveyed centre conductor for calibration at the 500 MHz frequency corresponding to the fundamental r.f. beam component.

It is of course fundamental to the accuracy with which the system measures the beam closed orbit relative to a survey mean orbit that an accurate figure for centre zero offset (δx_o and δy_o) is defined. A two stage procedure is proposed.

The F and D vessels will be mounted in a survey test rig and calibrated at low frequency (< 5 MHz) to avoid r.f. matching problems. This is possible if low capacitance, air space buttons are adopted as pick-up plates in the BPI and where coupling to the pick-up plates is defined by eqn.(1). The aim will be to define an accurate measurement centre relative to the survey

centre and to establish accurate Σ and Δ calibration. The signal processing hybrids will not be used.

The validity of this procedure was checked using the D vessel model assembly at a test frequency of 4.0 MHz. The microvolt level output signals from each pick-up plate were measured using an LF spectrum analyser and the beam position response was plotted (response plot 7). The composite coupling impedance response was also plotted using the following expression to define the high frequency (500 MHz) coupling impedance:

$$Z_c = \frac{1}{2}\left[\frac{|V_A|_m + |V_B|_m}{|V_g|_m}\right] \cdot \frac{f_{acc}}{f_m} \cdot Z_L \qquad (4)$$

where: Z_c : working frequency (f_{acc} = 500 MHz) composite coupling impedance

$|V_A|_m$ and $|V_B|_m$: plate outputs at test frequency (f_m = 4.0 MHz).

$|V_g|_m$: generator volts on test wire.

Z_L : characteristic impedance of the coaxial test assembly in the immediate region of the pick-up plates.

For comparison, and to confirm the general validity of the proposed procedure, the high frequency (f_{acc} = 500 MHz) monitor response previously measured in the same test rig and illustrated in response plot 3 is also shown in response plot 7. Within the limits of accuracy accepted in this initial test and in particular the relative accuracy with which the plate volts were measured at the two spot frequencies (500 MHz and 4.0 MHz), the general agreement is good. In the case of the beam position response, where the relative accuracy of measurement is not a factor, agreement is very good.

A second, and independent, stage of calibration will measure the characteristics of the F and D hybrid units. This will again involve calibration using a survey test rig but this time at a frequency of 500 MHz. The rig will incorporate short section model F and D head assemblies mounted to form

part of a matched coaxial test unit. The model BPI assemblies will be precision machined units and will serve as calibration standards for defining the centre zero offset of the hybrid units.

The overall accuracy of calibration will depend on a number of factors: calibration measurement error, mechanical errors in the calibration jig and survey errors. The calibration measurement error will dominate but, again because of the lower BPI calibration factors (C_x and C_y), the aim will be to achieve a reduction in the monitor error (≈ 0.25mm) currently specified for the installed stripline monitors.

5. TIMING SIGNAL PICK-UPS

Mounted as an integral part of each D-quadrupole BPI assembly are timing signal pick-up buttons. These are not specifically intended to be wideband beam diagnostic pick-ups but are installed to provide users with a source of unipolar beam derived timing signals during single bunch operation. The timing buttons incorporate ceramic spacers and, in the D-quadrupole BPI vessel, have the following characteristics:

Button diameter	= 14mm
Button capacitance C_p	≈ 7 pf
Low frequency 3 dB point f_c	≈ 450 MHz

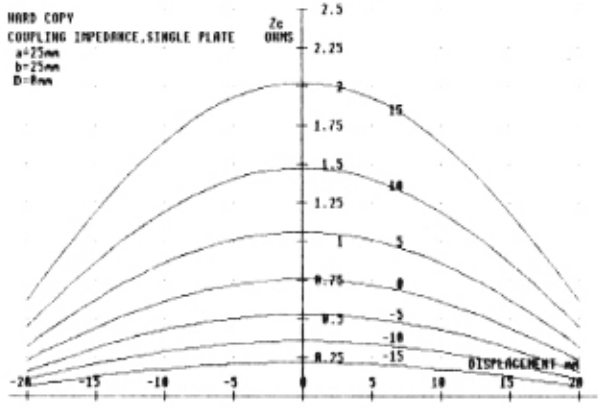

Fig.11. The Timing Button Coupling Response

The pulse response shown in fig.3 is for a test button assembly with similar frequency characteristics to the proposed timing signal pick-up. The coupling impedance response to a beam in the D vessel is shown in fig.11.

The response plot shows the variation of coupling impedance (Z_c) with horizontal beam displacement for different levels of vertical offset (0, ±5, ±10 ...mm). At beam centre the coupling impedance is ≈ 0.75 ohms.

In addition to providing users with timing signals, the timing buttons will also have some value when used as general beam diagnostic pick-ups. The pick-up is sensitive to vertical beam oscillations (Qv) but will have very low radial sensitivity. This implies that the timing buttons will have particular value for observing wideband beam structure and high frequency longitudinal beam components and will be a useful complement to the diagnostic stripline monitor presently installed in the SRS.

The upper frequency limit for application as a wideband beam diagnostics pick-up is determined by the geometry of the D-quadrupole vessel and the location of the button within the vessel. In practice, this upper limit is at a point somewhat below vessel cut-off and is dependent on the degree of isolation from local beam excited modes and edge effects. The location of the timing button within the D-quadrupole vessel provides the following:

Vessel cut-off ≈ 3 GHz

Isolation (assuming waveguide propagation) of local modes and edge effects > 20 dB at frequencies f_λ < 2 GHz.

6. ACKNOWLEDGEMENTS

Appreciation is due to Dr. D.E. Poole for support and helpful discussion. Grateful thanks are also due to Mr. M.J. Dufau for producing the computer response plots and to Mr. E.V. Carter for constructing the model BPI's and assisting with calibration.

REFERENCES

(1) G. Saxon, Daresbury Laboratory Report, DL/SCI/P374A, (1983).

(2) Synchrotron Radiation, appendix to the Daresbury Annual Report 1982/83.

(3) J. Borer et al, LEP-70/437, (1983).

APPENDIX 1

The Coupling Impedance of a Button Pick-up

Consider a single button pick-up mounted flush with the surface of a rectangular vessel

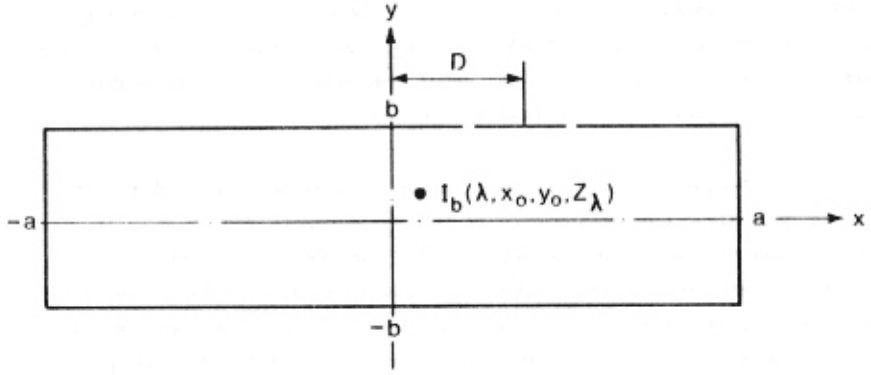

Fig. 1. Vessel geometry and beam coordinates

The surface charge induced on wall y = b has been calculated by Cuperus[1]:

$$\sigma_{y=b(x,z)} = \frac{-D_\lambda}{a} \cos\left[\frac{2\pi}{\lambda}(\upsilon t + Z_\lambda - Z)\right] \sum_{m=1}^{\infty} \frac{\sin\left[\frac{m\pi(a + x_o)}{2a}\right] \mathrm{sh}\left[\alpha_m(b + y_o)\right]}{\mathrm{sh}\,(2b\,\alpha_m)} \sin\left[\frac{m\pi(a + x)}{2a}\right]$$

where: D_λ = Amplitude of the Fourier beam component, wavelength λ, in C/m.

υ = particle beam velocity in Z direction

$$\alpha_m = \left[\left(\frac{2\pi}{\gamma\lambda}\right)^2 + \left(\frac{m\pi}{2a}\right)^2\right]^{1/2}$$

$$\gamma = \left[1 - \frac{\upsilon^2}{c^2}\right]^{-1/2}$$

In the case of both an ultra relativistic beam and a coaxial test line assembly γ tends to infinity

so $\alpha_m = \frac{m\pi}{2a}$

and $$\sigma_{y=b(x,z)} = \frac{-D_\lambda}{a} \cos\left[\frac{2\pi}{\lambda}(\upsilon t + Z_\lambda - Z)\right] \sum_{m=1}^{\infty} \beta_{m(x)} \qquad (1)$$

where: $$\beta_{m(x)} = \frac{\sin\left[\frac{m\pi(a + x_o)}{2a}\right] \mathrm{sh}\left[\frac{m\pi(b + y_o)}{2a}\right]}{\mathrm{sh}\left[\frac{m\pi b}{a}\right]} \sin\left[\frac{m\pi(a + x)}{2a}\right]$$

Button Current

Assuming a circular pick-up button at position D with surface area S and radius R:

If $a >> R << \lambda$

and I_λ = Amplitude of the Fourier beam component

$$= \upsilon D_\lambda = \lambda f_\lambda D_\lambda$$

Then the induced short circuit (Norton) current i_p is:

$$i_p = \frac{dq}{dt} = I_\lambda \frac{2\pi s}{\lambda a} \sin\left[\frac{2\pi}{\lambda}(\upsilon t + Z_\lambda)\right] \sum_{m=1}^{\infty} \beta_{m(x=D)} \qquad (2)$$

Coupling Impedance

If the plate is coupled directly to a terminated coaxial line then:

$$v_p = Z_p\, i_p$$

Where, if the plate is coupled through a high quality connector, Z_p can be considered as simply the composite impedance formed by the line impedance

Z_o in parallel with the reactive load presented by the plate capacitance C_p.

Now the coupling impedance of the pick-up plate is defined as:

$$Z_c = \frac{|V_p|}{I_\lambda}$$

and from eqns.(1) and (2):

a) When $\omega_\lambda Z_o C_p < 1$

$$Z_c = \frac{2\pi s}{\lambda a} Z_o \sum_{m=1}^{\infty} \beta_m{}_{(x = D)}$$

b) When $\omega_\lambda Z_o C_p > 1$

$$Z_c = \frac{s}{C_p a u} \sum_{m=1}^{\infty} \beta_m{}_{(x = D)}$$

REFERENCES

(1) J.H. Cuperus, Nucl. Instr. and Meth. 145 (1977) 219.

Response plot 1

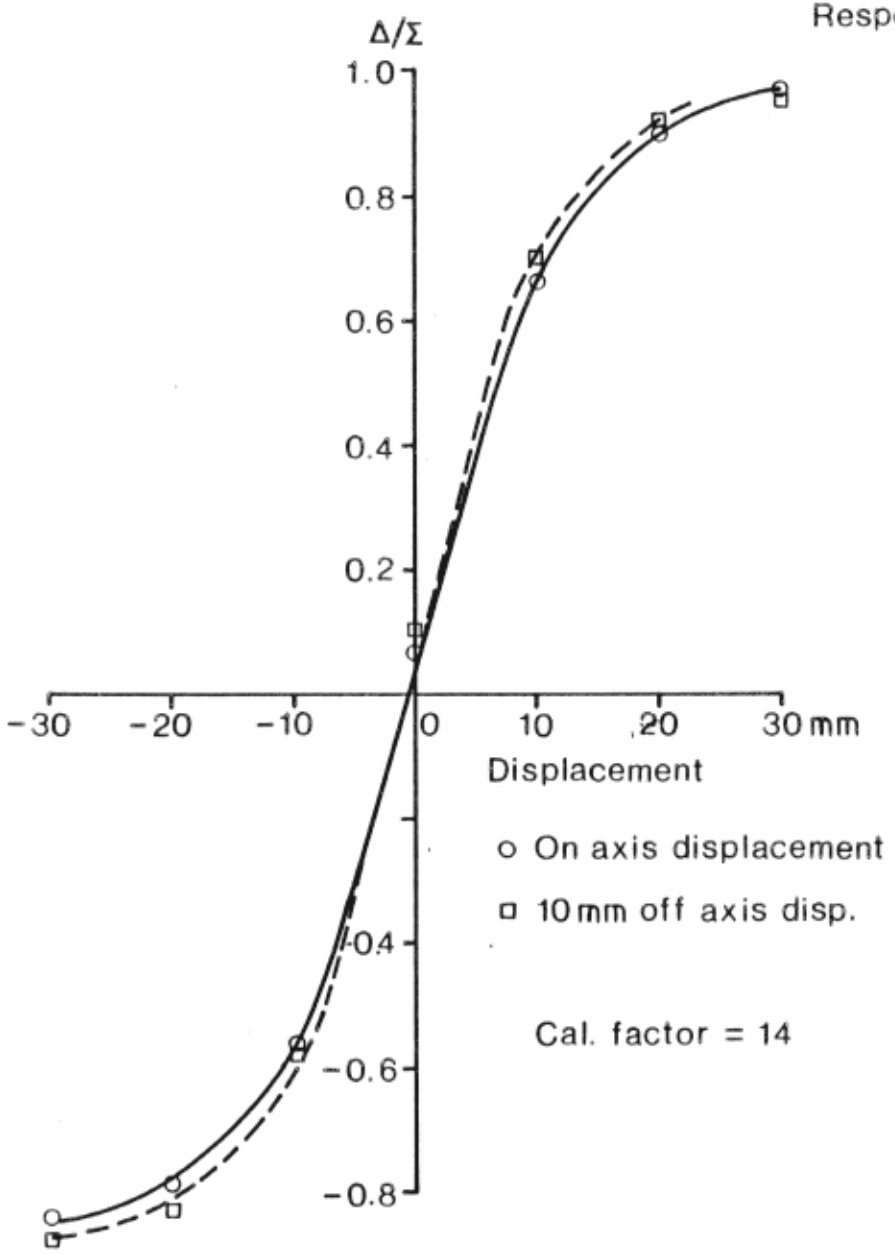

Processed BPI response

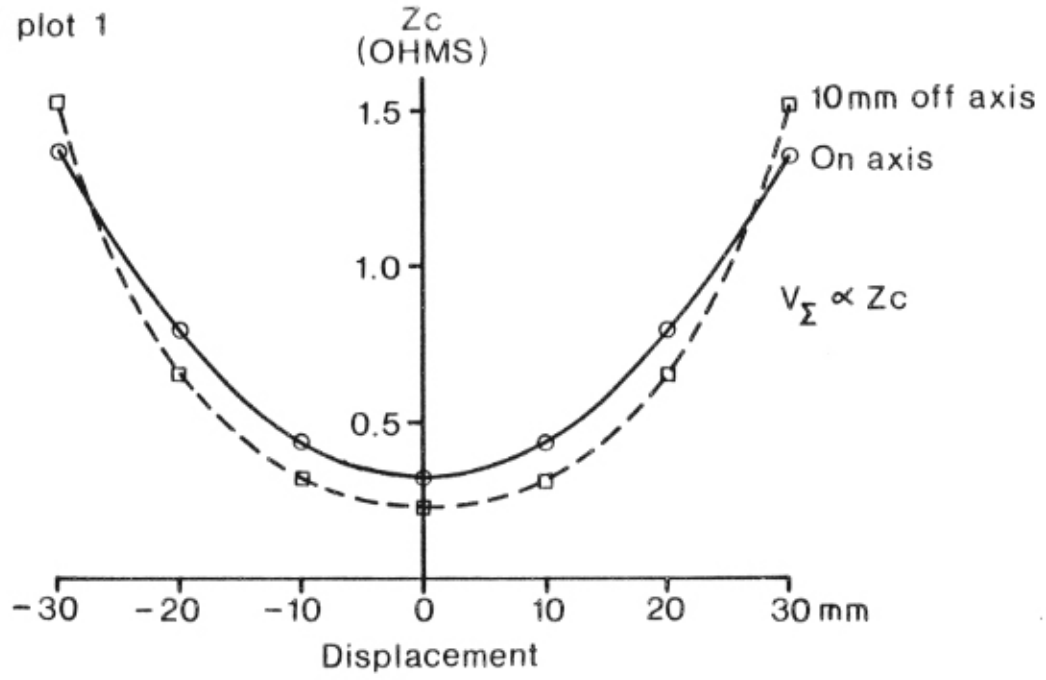

Total current response

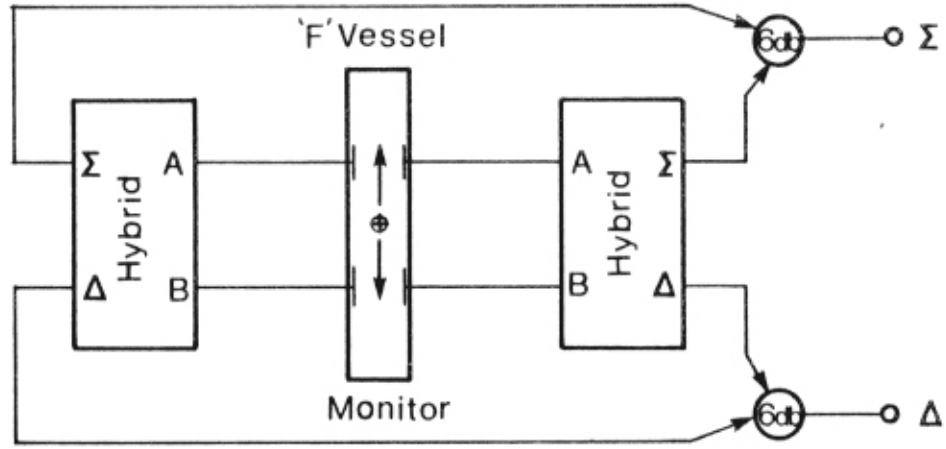

'F' Vessel model BPI: Capacitive button pick-ups

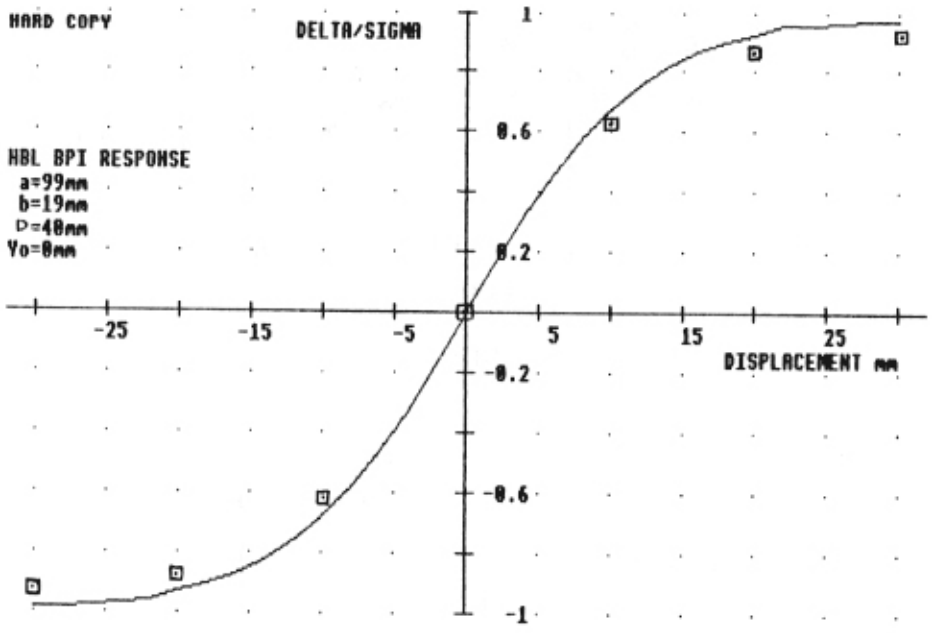

□ : MEASURED RESPONSE

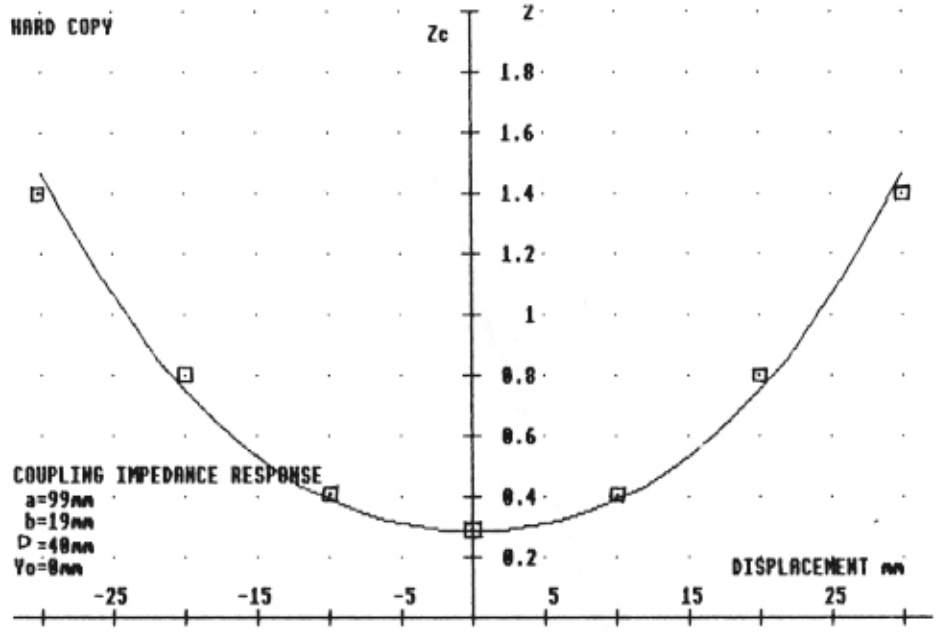

RESPONSE PLOT 2

Response plot 3

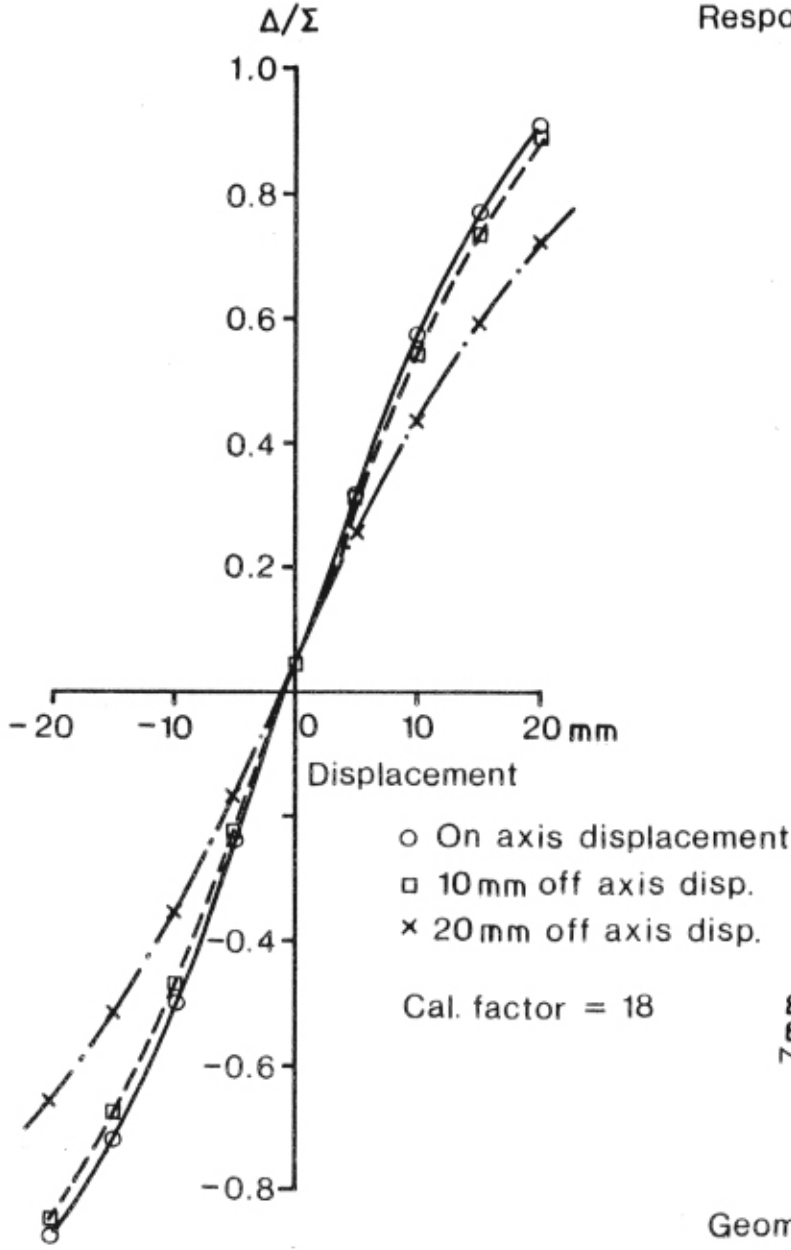

Processed BPI response

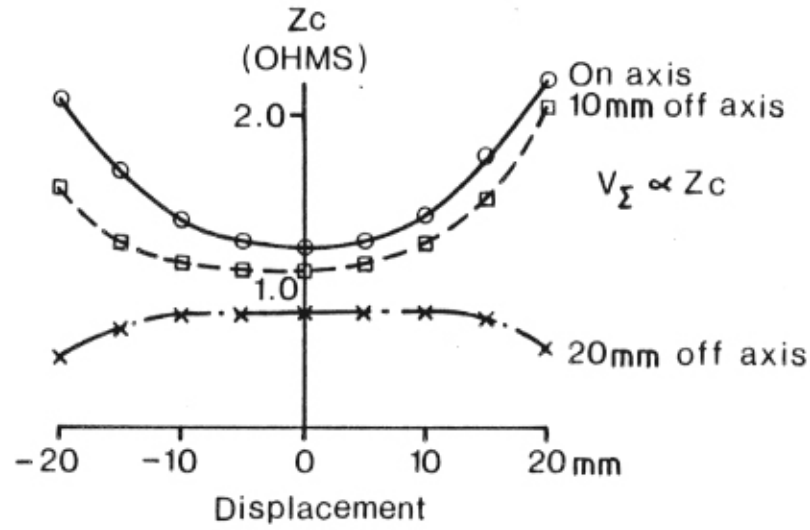

Total current response

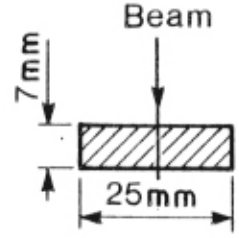

Geometry of pick-up plate

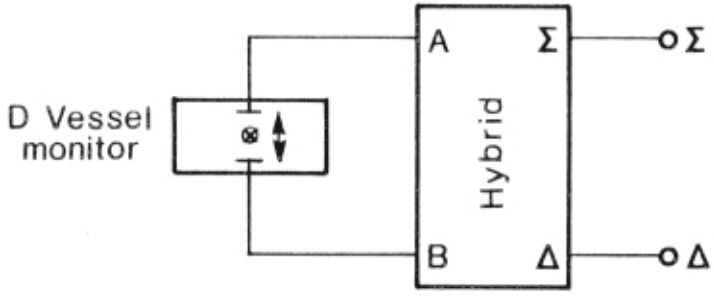

'D' Vessel model BPI: Two on-axis capacitive pick-up plates

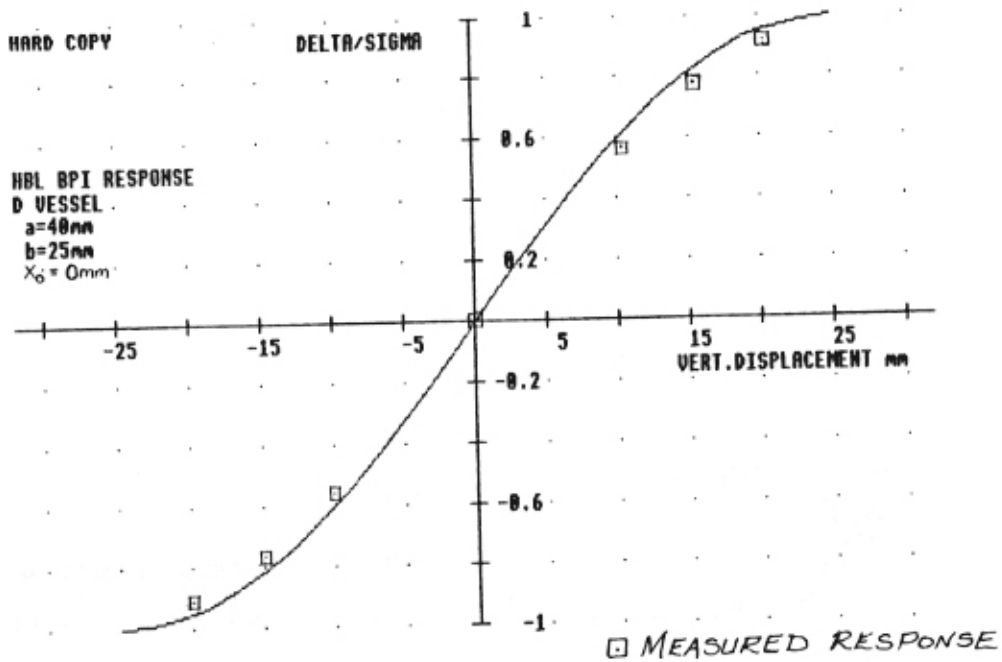

⊡ MEASURED RESPONSE

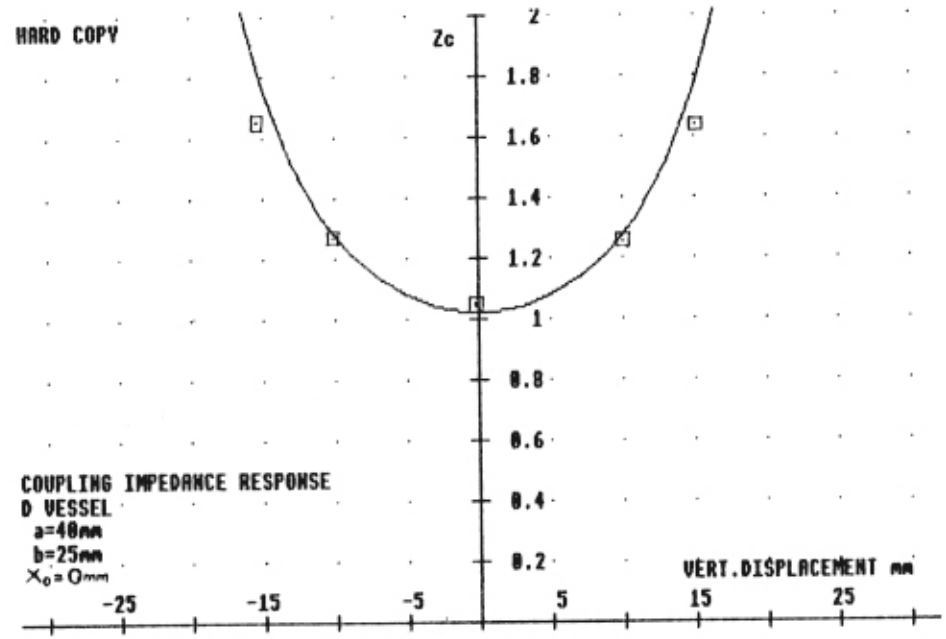

RESPONSE PLOT 4

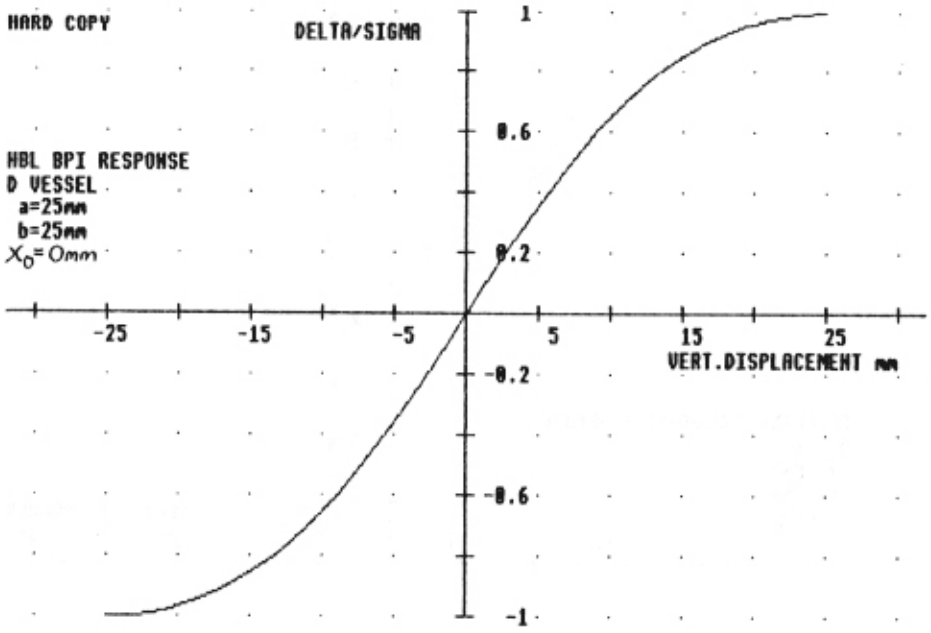

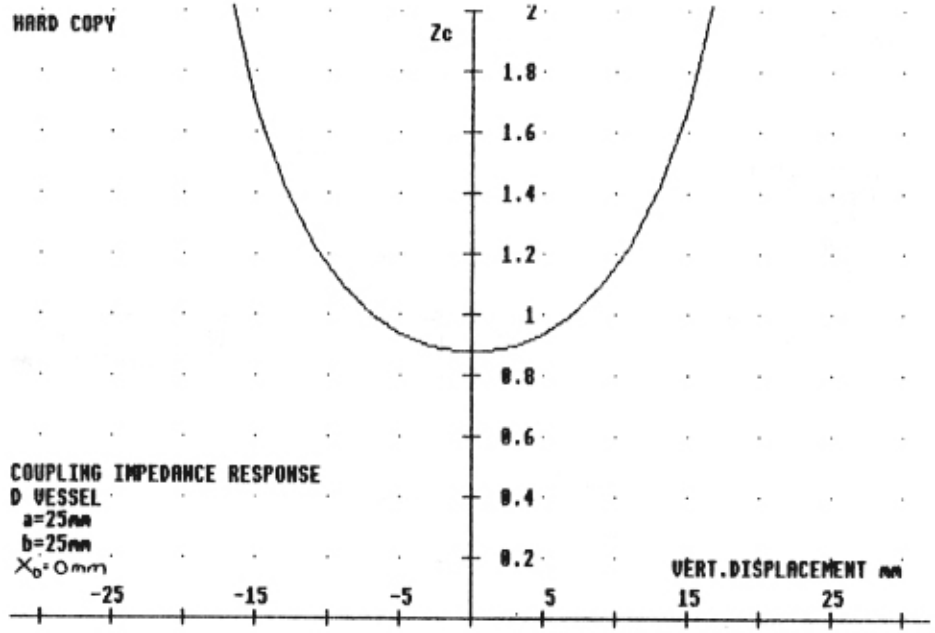

RESPONSE PLOT 5

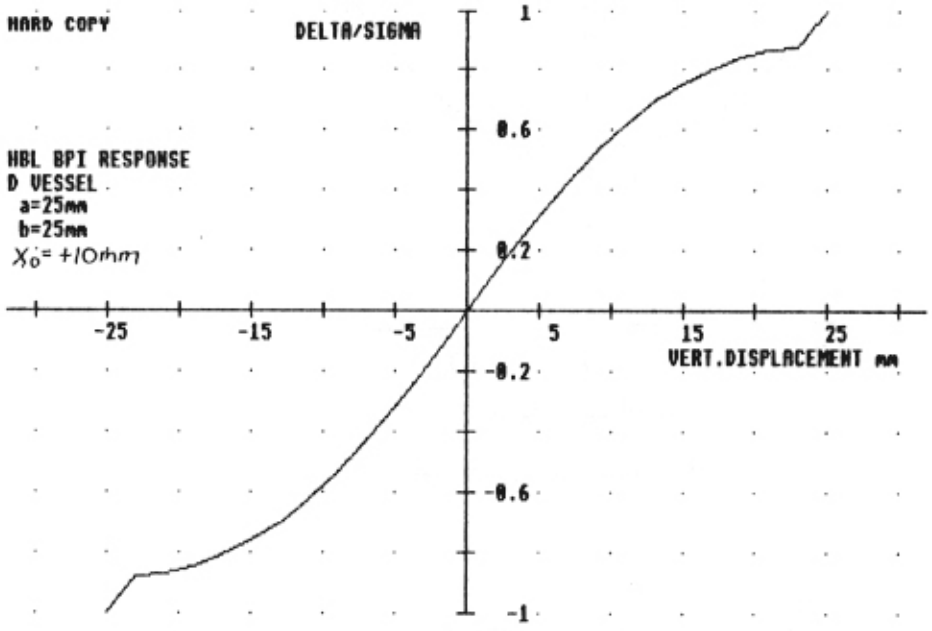

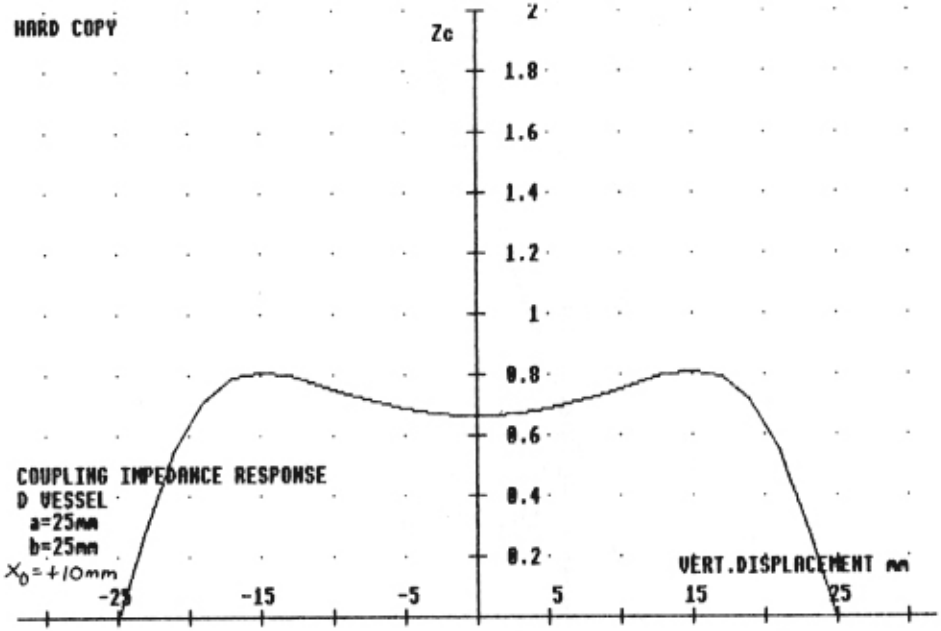

RESPONSE PLOT 6

Response plot 7

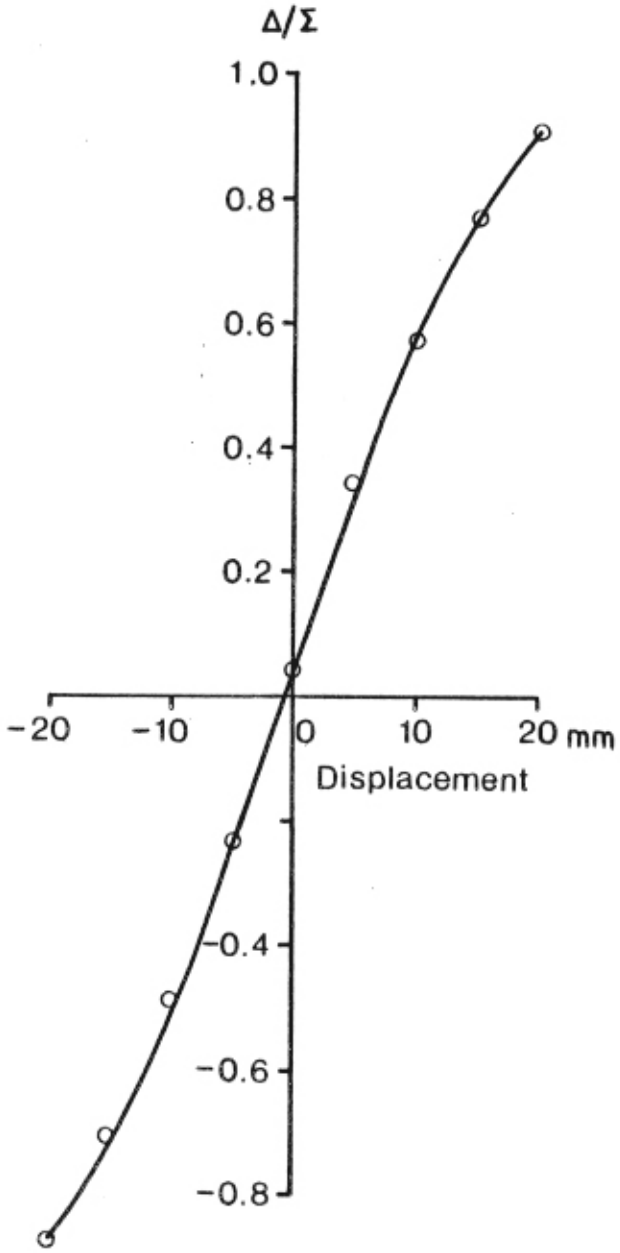

Beam position response

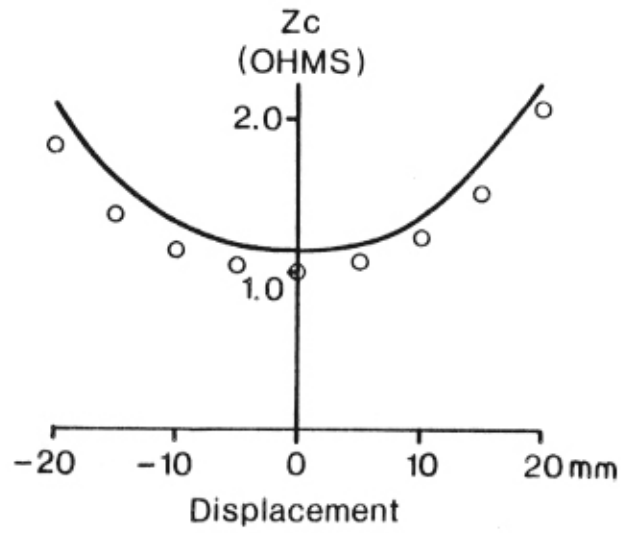

Total current response

○ Low frequency (4·0MHz) measurement points

—— High frequency (500MHz) response

'D' Vessel model BP1: Low frequency calibration response